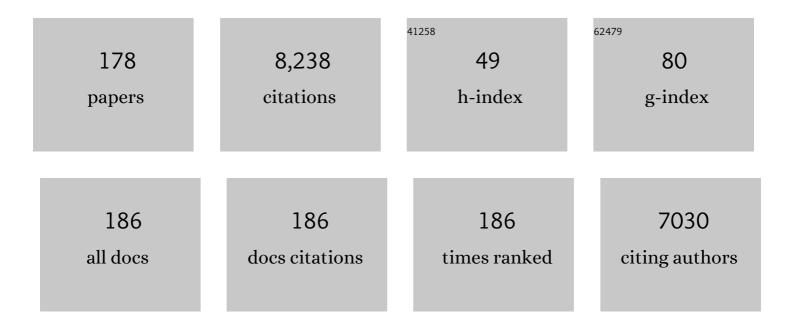
Sharon Ashbrook

List of Publications by Year in descending order

Source: https://exaly.com/author-pdf/4568499/publications.pdf Version: 2024-02-01



#	Article	IF	CITATIONS
1	Origin of the temperature dependence of ¹³ C pNMR shifts for copper paddlewheel MOFs. Chemical Science, 2022, 13, 2674-2685.	3.7	2
2	Solid-state NMR spectroscopy. Nature Reviews Methods Primers, 2021, 1, .	11.8	196
3	Thermal Dehydrofluorination of GaPO-34 Revealed by NMR Crystallography. Journal of Physical Chemistry C, 2021, 125, 2537-2545.	1.5	5
4	¹⁷ 0 NMR spectroscopy of crystalline microporous materials. Chemical Science, 2021, 12, 5016-5036.	3.7	33
5	Exploring cation disorder in mixedâ€metal pyrochlore ceramics using ¹⁷ 0 NMR spectroscopy and firstâ€principles calculations. Magnetic Resonance in Chemistry, 2021, 59, 961-974.	1.1	0
6	Recent advances in solidâ€state nuclear magnetic resonance spectroscopy of quadrupolar nuclei. Magnetic Resonance in Chemistry, 2021, 59, 851-852.	1.1	1
7	Single-step synthesis and interface tuning of core–shell metal–organic framework nanoparticles. Chemical Science, 2021, 12, 4494-4502.	3.7	11
8	Formation Mechanism and Porosity Development in Porous Boron Nitride. Journal of Physical Chemistry C, 2021, 125, 27429-27439.	1.5	15
9	Facile, Room-Temperature ¹⁷ O Enrichment of Zeolite Frameworks Revealed by Solid-State NMR Spectroscopy. Journal of the American Chemical Society, 2020, 142, 900-906.	6.6	48
10	Phase Distribution, Composition, and Disorder in Y ₂ (Hf,Sn) ₂ O ₇ Ceramics: Insights from Solid-State NMR Spectroscopy and First-Principles Calculations. Journal of Physical Chemistry C, 2020, 124, 17073-17084.	1.5	7
11	Solid-state host–guest influences on a BODIPY dye hosted within a crystalline sponge. New Journal of Chemistry, 2020, 44, 14108-14115.	1.4	6
12	Application of NMR Crystallography to Highly Disordered Templated Materials: Extensive Local Structural Disorder in the Gallophosphate GaPO-34A. Inorganic Chemistry, 2020, 59, 11616-11626.	1.9	9
13	Site‧pecific Iron Substitution in STAâ€28, a Large Pore Aluminophosphate Zeotype Prepared by Using 1,10â€Phenanthrolines as Frameworkâ€Bound Templates. Angewandte Chemie - International Edition, 2020, 59, 15186-15190.	7.2	4
14	Synthesis of Chiral MOFâ€74 Frameworks by Postâ€5ynthetic Modification by Using an Amino Acid. Chemistry - A European Journal, 2020, 26, 13957-13965.	1.7	35
15	Mechanochemically assisted hydrolysis in the ADOR process. Chemical Science, 2020, 11, 7060-7069.	3.7	12
16	Site‣pecific Iron Substitution in STAâ€28, a Large Pore Aluminophosphate Zeotype Prepared by Using 1,10â€Phenanthrolines as Frameworkâ€Bound Templates. Angewandte Chemie, 2020, 132, 15298-15302.	1.6	2
17	Following the unusual breathing behaviour of ¹⁷ O-enriched mixed-metal (Al,Ga)-MIL-53 using NMR crystallography. Physical Chemistry Chemical Physics, 2020, 22, 14514-14526.	1.3	16
18	Synthesis and Polymorphism of Mixed Aluminum–Gallium Oxides. Inorganic Chemistry, 2020, 59, 3805-3816.	1.9	28

#	Article	IF	CITATIONS
19	Phosphorus–Bismuth <i>Peri</i> -Substituted Acenaphthenes: A Synthetic, Structural, and Computational Study. Inorganic Chemistry, 2020, 59, 5616-5625.	1.9	13
20	Fast room temperature lability of aluminosilicate zeolites. Nature Communications, 2019, 10, 4690.	5.8	75
21	Ensemble-Based Modeling of the NMR Spectra of Solid Solutions: Cation Disorder in Y ₂ (Sn,Ti) ₂ O ₇ . Journal of the American Chemical Society, 2019, 141, 17838-17846.	6.6	29
22	NMR spectroscopy of paramagnetic solids. Solid State Nuclear Magnetic Resonance, 2019, 104, 101625.	1.5	1
23	Visualization of the effect of additives on the nanostructures of individual bio-inspired calcite crystals. Chemical Science, 2019, 10, 1176-1185.	3.7	26
24	A Picture of Disorder in Hydrous Wadsleyite—Under the Combined Microscope of Solid-State NMR Spectroscopy and Ab Initio Random Structure Searching. Journal of the American Chemical Society, 2019, 141, 3024-3036.	6.6	13
25	STA-27, a porous Lewis acidic scandium MOF with an unexpected topology type prepared with 2,3,5,6-tetrakis(4-carboxyphenyl)pyrazine. Journal of Materials Chemistry A, 2019, 7, 5685-5701.	5.2	22
26	A procedure for identifying possible products in the assembly–disassembly–organization–reassembly (ADOR) synthesis of zeolites. Nature Protocols, 2019, 14, 781-794.	5.5	22
27	13C pNMR of "crumple zone―Cu(II) isophthalate metal-organic frameworks. Solid State Nuclear Magnetic Resonance, 2019, 101, 44-50.	1.5	11
28	NMR chemical shifts of urea loaded copper benzoate. A joint solid-state NMR and DFT study. Solid State Nuclear Magnetic Resonance, 2019, 101, 31-37.	1.5	17
29	Sensitivity improvement in 5QMAS NMR experiments using FAM-N pulses. Solid State Nuclear Magnetic Resonance, 2019, 100, 1-10.	1.5	3
30	Nuclear Magnetic Resonance Spectroscopy as a Dynamical Structural Probe of Hydrogen under High Pressure. Physical Review Letters, 2019, 122, 135501.	2.9	9
31	Rationalization of solid-state NMR multi-pulse decoupling strategies: Coupling of spin l = ½ and half-integer quadrupolar nuclei. Journal of Magnetic Resonance, 2019, 303, 48-56.	1.2	3
32	Kinetics and Mechanism of the Hydrolysis and Rearrangement Processes within the Assembly–Disassembly–Organization–Reassembly Synthesis of Zeolites. Journal of the American Chemical Society, 2019, 141, 4453-4459.	6.6	21
33	Is the <scp>³¹P</scp> chemical shift anisotropy of aluminophosphates a useful parameter for <scp>NMR</scp> crystallography?. Magnetic Resonance in Chemistry, 2019, 57, 176-190.	1.1	6
34	¹⁷ O solid-state NMR spectroscopy of A ₂ B ₂ O ₇ oxides: quantitative isotopic enrichment and spectral acquisition?. RSC Advances, 2018, 8, 7089-7101.	1.7	13
35	Modulatorâ€Controlled Synthesis of Microporous STAâ€26, an Interpenetrated 8,3â€Connected Zirconium MOF with the <i>theâ€i</i> Topology, and its Reversible Lattice Shift. Chemistry - A European Journal, 2018, 24, 6115-6126.	1.7	23
36	Recent Advances in Solid-State Nuclear Magnetic Resonance Spectroscopy. Annual Review of Analytical Chemistry, 2018, 11, 485-508.	2.8	45

#	Article	IF	CITATIONS
37	Cost-effective ¹⁷ O enrichment and NMR spectroscopy of mixed-metal terephthalate metal–organic frameworks. Chemical Science, 2018, 9, 850-859.	3.7	49
38	Pressure-induced chemistry for the 2D to 3D transformation of zeolites. Journal of Materials Chemistry A, 2018, 6, 5255-5259.	5.2	21
39	A Bifunctional MOF Catalyst Containing Metal–Phosphine and Lewis Acidic Active Sites. Chemistry - A European Journal, 2018, 24, 15309-15318.	1.7	40
40	SERS of Trititanate Nanotubes: Selective Enhancement of Catechol Compounds. ChemistrySelect, 2018, 3, 8338-8343.	0.7	3
41	Perspective: Current advances in solid-state NMR spectroscopy. Journal of Chemical Physics, 2018, 149, 040901.	1.2	28
42	Polymorphism, Weak Interactions and Phase Transitions in Chalcogen–Phosphorus Heterocycles. Chemistry - A European Journal, 2018, 24, 11067-11081.	1.7	4
43	An expanded MIL-53-type coordination polymer with a reactive pendant ligand. CrystEngComm, 2018, 20, 4355-4358.	1.3	5
44	Hydrolytic stability in hemilabile metal–organic frameworks. Nature Chemistry, 2018, 10, 1096-1102.	6.6	134
45	Alkaline-Earth Rhodium Hydroxides: Synthesis, Structures, and Thermal Decomposition to Complex Oxides. Inorganic Chemistry, 2018, 57, 11217-11224.	1.9	8
46	Synthesis of ZIFâ€93/11 Hybrid Nanoparticles via Postâ€5ynthetic Modification of ZIFâ€93 and Their Use for H ₂ /CO ₂ Separation. Chemistry - A European Journal, 2018, 24, 11211-11219.	1.7	27
47	Investigating FAM-N pulses for signal enhancement in MQMAS NMR of quadrupolar nuclei. Solid State Nuclear Magnetic Resonance, 2017, 84, 89-102.	1.5	9
48	Porous zinc and cobalt 2-nitroimidazolate frameworks with six-membered ring windows and a layered cobalt 2-nitroimidazolate polymorph. CrystEngComm, 2017, 19, 1377-1388.	1.3	6
49	A Multinuclear NMR Study of Six Forms of AlPO-34: Structure and Motional Broadening. Journal of Physical Chemistry C, 2017, 121, 1781-1793.	1.5	25
50	Exploiting NMR spectroscopy for the study of disorder in solids. International Reviews in Physical Chemistry, 2017, 36, 39-115.	0.9	65
51	Selective Oxidation and Functionalization of 6-Diphenylphosphinoacenaphthyl-5-tellurenyl Species 6-Ph ₂ P-Ace-5-TeX (X = Mes, Cl, O ₃ SCF ₃). Various Types of P–E···Te(II,IV) Bonding Situations (E = O, S, Se). Organometallics, 2017, 36, 1566-1579.	1.1	18
52	In situ solid-state NMR and XRD studies of the ADOR process and the unusual structure of zeolite IPC-6. Nature Chemistry, 2017, 9, 1012-1018.	6.6	63
53	An NMR Crystallographic Investigation of the Relationships between the Crystal Structure and ²⁹ Si Isotropic Chemical Shift in Silica Zeolites. Journal of Physical Chemistry C, 2017, 121, 15198-15210.	1.5	28
54	Solidâ€State NMR Spectroscopy Proves the Presence of Pentaâ€coordinated Sc Sites in MILâ€100(Sc). Chemistry - A European Journal, 2017, 23, 9525-9534.	1.7	19

#	Article	IF	CITATIONS
55	Synthesis, Isotopic Enrichment, and Solid-State NMR Characterization of Zeolites Derived from the Assembly, Disassembly, Organization, Reassembly Process. Journal of the American Chemical Society, 2017, 139, 5140-5148.	6.6	42
56	Determining the Surface Structure of Silicated Alumina Catalysts via Isotopic Enrichment and Dynamic Nuclear Polarization Surface-Enhanced NMR Spectroscopy. Journal of Physical Chemistry C, 2017, 121, 22977-22984.	1.5	34
57	Calculation and experimental measurement of paramagnetic NMR parameters of phenolic oximate Cu(<scp>ii</scp>) complexes. Chemical Communications, 2017, 53, 10512-10515.	2.2	11
58	Investigation of zeolitic imidazolate frameworks using 13 C and 15 N solid-state NMR spectroscopy. Solid State Nuclear Magnetic Resonance, 2017, 87, 54-64.	1.5	21
59	Effects of Extraframework Species on the Structure-Based Prediction of ³¹ P Isotropic Chemical Shifts of Aluminophosphates. Journal of Physical Chemistry C, 2017, 121, 28065-28076.	1.5	12
60	Ionothermal synthesis and characterization of CoAPO-34 molecular sieve. Microporous and Mesoporous Materials, 2017, 239, 336-341.	2.2	17
61	A gel aging effect in the synthesis of open-framework gallium phosphates: structure solution and solid-state NMR of a large-pore, open-framework material. Dalton Transactions, 2017, 46, 16895-16904.	1.6	4
62	The ambient hydration of the aluminophosphate JDF-2 to AlPO-53(A): insights from NMR crystallography. Acta Crystallographica Section C, Structural Chemistry, 2017, 73, 191-201.	0.2	6
63	Combining solid-state NMR spectroscopy with first-principles calculations – a guide to NMR crystallography. Chemical Communications, 2016, 52, 7186-7204.	2.2	202
64	Paramagnetic NMR of Phenolic Oxime Copper Complexes: A Joint Experimental and Density Functional Study. Chemistry - A European Journal, 2016, 22, 15328-15339.	1.7	22
65	Exploring the self-assembly and energy transfer of dynamic supramolecular iridium-porphyrin systems. Dalton Transactions, 2016, 45, 17195-17205.	1.6	23
66	Phase Composition and Disorder in La ₂ (Sn,Ti) ₂ O ₇ Ceramics: New Insights from NMR Crystallography. Journal of Physical Chemistry C, 2016, 120, 20288-20296.	1.5	15
67	Investigating Unusual Homonuclear Intermolecular "Through-Space―J Couplings in Organochalcogen Systems. Inorganic Chemistry, 2016, 55, 10881-10887.	1.9	15
68	Hunting for hydrogen: random structure searching and prediction of NMR parameters of hydrous wadsleyite. Physical Chemistry Chemical Physics, 2016, 18, 10173-10181.	1.3	19
69	Inside Cover: Conformational Dependence of Throughâ€Space Tellurium–Tellurium Spin–Spin Coupling in <i>Peri</i> â€Substituted Bis(Tellurides) (Chem. Eur. J. 9/2015). Chemistry - A European Journal, 2015, 21, 3506-3506.	1.7	0
70	[1,2,5]Selenadiazolo[3,4â€ <i>b</i>]pyrazines: Synthesis from 3,4â€Diaminoâ€1,2,5â€selenaÂdiazole and Gener of Persistent Radical Anions. European Journal of Organic Chemistry, 2015, 2015, 5585-5593.	ation 1.2	18
71	New insights into phase distribution, phase composition and disorder in Y ₂ (Zr,Sn) ₂ O ₇ ceramics from NMR spectroscopy. Physical Chemistry Chemical Physics, 2015, 17, 9049-9059.	1.3	22
72	Conformational Dependence of Throughâ€Space Tellurium–Tellurium Spin–Spin Coupling in <i>Peri</i> â€Substituted Bis(Tellurides). Chemistry - A European Journal, 2015, 21, 3613-3627.	1.7	19

#	Article	IF	CITATIONS
73	<i>Peri</i> -Substituted Phosphorus–Tellurium Systems–An Experimental and Theoretical Investigation of the P···Te through-Space Interaction. Inorganic Chemistry, 2015, 54, 2435-2446.	1.9	30
74	Unusual Intermolecular "Through-Space― <i>J</i> Couplings in P–Se Heterocycles. Journal of the American Chemical Society, 2015, 137, 6172-6175.	6.6	24
75	Exploiting Synthetic Conditions to Promote Structural Diversity within the Scandium(III)/Pyrimidine-4,6-dicarboxylate System. Crystal Growth and Design, 2015, 15, 2352-2363.	1.4	31
76	Post-synthetic modification of zinc metal-organic frameworks through palladium-catalysed carbon–carbon bond formation. Journal of Organometallic Chemistry, 2015, 792, 134-138.	0.8	4
77	An NMR crystallographic approach to monitoring cation substitution in the aluminophosphate STA-2. Solid State Nuclear Magnetic Resonance, 2015, 65, 64-74.	1.5	14
78	Solid-state NMR measurements and DFT calculations of the magnetic shielding tensors of protons of water trapped in barium chlorate monohydrate. RSC Advances, 2014, 4, 56248-56258.	1.7	17
79	Mixedâ€Metal MILâ€100(Sc,M) (M=Al, Cr, Fe) for Lewis Acid Catalysis and Tandem CC Bond Formation and Alcohol Oxidation. Chemistry - A European Journal, 2014, 20, 17185-17197.	1.7	104
80	Sterically Restricted Tin Phosphines, Stabilized by Weak Intramolecular Donor–Acceptor Interactions. Organometallics, 2014, 33, 2424-2433.	1.1	18
81	Probing interactions through space using spin–spin coupling. Dalton Transactions, 2014, 43, 6548-6560.	1.6	28
82	A Modular Approach for the Synthesis of Nanometer-Sized Polynitroxide Multi-Spin Systems. Journal of Organic Chemistry, 2014, 79, 8313-8323.	1.7	13
83	New Methods and Applications in Solid-State NMR Spectroscopy of Quadrupolar Nuclei. Journal of the American Chemical Society, 2014, 136, 15440-15456.	6.6	120
84	Calculating NMR parameters in aluminophosphates: evaluation of dispersion correction schemes. Physical Chemistry Chemical Physics, 2014, 16, 2660.	1.3	32
85	Recent developments in solid-state NMR spectroscopy of crystalline microporous materials. Physical Chemistry Chemical Physics, 2014, 16, 8223-8242.	1.3	69
86	Investigating Relationships between the Crystal Structure and ³¹ P Isotropic Chemical Shifts in Calcined Aluminophosphates. Journal of Physical Chemistry C, 2014, 118, 23285-23296.	1.5	23
87	Efficient Amplitude-Modulated Pulses for Triple- to Single-Quantum Coherence Conversion in MQMAS NMR. Journal of Physical Chemistry A, 2014, 118, 6018-6025.	1.1	19
88	Zeolites with Continuously Tuneable Porosity. Angewandte Chemie - International Edition, 2014, 53, 13210-13214.	7.2	104
89	Characterization of Structural Disorder in γ-Ga ₂ O ₃ . Journal of Physical Chemistry C, 2014, 118, 16188-16198.	1.5	107
90	Multirate delivery of multiple therapeutic agents from metal-organic frameworks. APL Materials, 2014, 2, .	2.2	58

#	Article	IF	CITATIONS
91	Solid-State NMR of High-Pressure Silicates in the Earth's Mantle. Annual Reports on NMR Spectroscopy, 2013, 79, 241-332.	0.7	11
92	Unusual Phase Behavior in the Piezoelectric Perovskite System, LixNa1–xNbO3. Inorganic Chemistry, 2013, 52, 8872-8880.	1.9	31
93	Investigation of the hydrothermal crystallisation of the perovskite solid solution NaCe1â [~] La Ti2O6 and its defect chemistry. Journal of Solid State Chemistry, 2013, 207, 117-125.	1.4	8
94	Application of NMR crystallography to the determination of the mechanism of charge-balancing in organocation-templated AlPO STA-2. CrystEngComm, 2013, 15, 8668.	1.3	28
95	Structural Study of La _{1–<i>x</i>} Y _{<i>x</i>} ScO ₃ , Combining Neutron Diffraction, Solid-State NMR, and First-Principles DFT Calculations. Journal of Physical Chemistry C, 2013, 117, 2252-2265.	1.5	39
96	Exploiting Periodic First-Principles Calculations in NMR Spectroscopy of Disordered Solids. Accounts of Chemical Research, 2013, 46, 1964-1974.	7.6	53
97	High-resolution solid-state 13C NMR spectroscopy of the paramagnetic metal–organic frameworks, STAM-1 and HKUST-1. Physical Chemistry Chemical Physics, 2013, 15, 919-929.	1.3	64
98	The pyrochlore to defect fluorite phase transition in Y2Sn2â^'xZrxO7. RSC Advances, 2013, 3, 5090.	1.7	55
99	A family of zeolites with controlled pore size prepared using a top-down method. Nature Chemistry, 2013, 5, 628-633.	6.6	355
100	Color and Brightness Tuning in Heteronuclear Lanthanide Terephthalate Coordination Polymers. European Journal of Inorganic Chemistry, 2013, 2013, 3464-3476.	1.0	76
101	Water in the Earth's mantle: a solid-state NMR study of hydrous wadsleyite. Chemical Science, 2013, 4, 1523.	3.7	41
102	First-Principles Calculation of NMR Parameters Using the Gauge Including Projector Augmented Wave Method: A Chemist's Point of View. Chemical Reviews, 2012, 112, 5733-5779.	23.0	446
103	A novel structural form of MIL-53 observed for the scandium analogue and its response to temperature variation and CO ₂ adsorption. Dalton Transactions, 2012, 41, 3937-3941.	1.6	95
104	Applications of NMR Crystallography to Problems in Biomineralization: Refinement of the Crystal Structure and ³¹ P Solid-State NMR Spectral Assignment of Octacalcium Phosphate. Journal of the American Chemical Society, 2012, 134, 12508-12515.	6.6	80
105	A Multinuclear Solid-State NMR Study of Templated and Calcined Chabazite-Type GaPO-34. Journal of Physical Chemistry C, 2012, 116, 15048-15057.	1.5	24
106	Ionothermal 17O enrichment of oxides using microlitre quantities of labelled water. Chemical Science, 2012, 3, 2293.	3.7	57
107	Exploiting the Chemical Shielding Anisotropy to Probe Structure and Disorder in Ceramics: 89Y MAS NMR and First-Principles Calculations. Journal of Physical Chemistry C, 2012, 116, 4273-4286.	1.5	41
108	Noncovalent Interactions in Peri-Substituted Chalconium Acenaphthene and Naphthalene Salts: A Combined Experimental, Crystallographic, Computational, and Solid-State NMR Study. Inorganic Chemistry, 2012, 51, 11087-11097.	1.9	38

#	Article	IF	CITATIONS
109	New Twists on the Perovskite Theme: Crystal Structures of the Elusive Phases R and S of NaNbO ₃ . Inorganic Chemistry, 2012, 51, 6876-6889.	1.9	78
110	Synthesis and crystal chemistry of the STA-12 family of metal N,N′-piperazinebis(methylenephosphonate)s and applications of STA-12(Ni) in the separation of gases. Microporous and Mesoporous Materials, 2012, 157, 3-17.	2.2	49
111	Towards homonuclear J solid-state NMR correlation experiments for half-integer quadrupolar nuclei: experimental and simulated 11B MAS spin-echo dephasing and calculated 2JBB coupling constants for lithium diborate. Physical Chemistry Chemical Physics, 2011, 13, 5778.	1.3	34
112	77Se Solid-State NMR of Inorganic and Organoselenium Systems: A Combined Experimental and Computational Study. Journal of Physical Chemistry C, 2011, 115, 10859-10872.	1.5	25
113	Synthesis and characterization of hybrid organic/inorganic nanotubes of the imogolite type and their behaviour towards methane adsorption. Physical Chemistry Chemical Physics, 2011, 13, 744-750.	1.3	102
114	93Nb NMR and DFT investigation of the polymorphs of NaNbO3. Physical Chemistry Chemical Physics, 2011, 13, 7565.	1.3	50
115	¹¹⁹ Sn MAS NMR and first-principles calculations for the investigation of disorder in stannate pyrochlores. Physical Chemistry Chemical Physics, 2011, 13, 488-497.	1.3	49
116	Structural Chemistry, Monoclinic-to-Orthorhombic Phase Transition, and CO ₂ Adsorption Behavior of the Small Pore Scandium Terephthalate, Sc ₂ (O ₂ CC ₆ H ₄ CO ₂) ₃ , and Its Nitro- And Amino-Functionalized Derivatives. Inorganic Chemistry, 2011, 50, 10844-10858.	1.9	75
117	Protecting group and switchable pore-discriminating adsorption properties of a hydrophilic–hydrophobic metal–organic framework. Nature Chemistry, 2011, 3, 304-310.	6.6	141
118	Observation of "hidden―magnesium: First-principles calculations and 25Mg solid-state NMR of enstatite. Solid State Nuclear Magnetic Resonance, 2011, 40, 91-99.	1.5	25
119	A co-templating route to the synthesis of Cu SAPO STA-7, giving an active catalyst for the selective catalytic reduction of NO. Microporous and Mesoporous Materials, 2011, 146, 36-47.	2.2	44
120	Octaselenocyclododecane. Angewandte Chemie - International Edition, 2011, 50, 4123-4126.	7.2	23
121	Synthesis, characterisation and adsorption properties of microporous scandium carboxylates with rigid and flexible frameworks. Microporous and Mesoporous Materials, 2011, 142, 322-333.	2.2	170
122	Detecting solid-state reactivity in 10-hydroxy-10,9-boroxophenanthrene using NMR spectroscopy. Tetrahedron, 2010, 66, 6238-6250.	1.0	21
123	Molecular Modeling, Multinuclear NMR, and Diffraction Studies in the Templated Synthesis and Characterization of the Aluminophosphate Molecular Sieve STA-2. Journal of Physical Chemistry C, 2010, 114, 12698-12710.	1.5	44
124	The Polar Phase of NaNbO ₃ : A Combined Study by Powder Diffraction, Solid-State NMR, and First-Principles Calculations. Journal of the American Chemical Society, 2010, 132, 8732-8746.	6.6	178
125	High-Resolution ¹⁹ F MAS NMR Spectroscopy: Structural Disorder and Unusual <i>J</i> Couplings in a Fluorinated Hydroxy-Silicate. Journal of the American Chemical Society, 2010, 132, 15651-15660.	6.6	83
126	Task specific ionic liquids for the ionothermal synthesis of siliceous zeolites. Chemical Science, 2010, 1, 483.	3.7	81

#	Article	IF	CITATIONS
127	Dynamics on the microsecond timescale in hydrous silicates studied by solid-state 2H NMR spectroscopy. Physical Chemistry Chemical Physics, 2010, 12, 2989.	1.3	30
128	Novel Large-Pore Aluminophosphate Molecular Sieve STA-15 Prepared Using the Tetrapropylammonium Cation As a Structure Directing Agent. Chemistry of Materials, 2010, 22, 338-346.	3.2	35
129	Structure and NMR assignment in AlPO4-15: A combined study by diffraction, MAS NMR and first-principles calculations. Solid State Sciences, 2009, 11, 1001-1006.	1.5	38
130	Second-order cross-term interactions in high-resolution MAS NMR of quadrupolar nuclei. Progress in Nuclear Magnetic Resonance Spectroscopy, 2009, 55, 160-181.	3.9	28
131	Solid-State 170 NMR Spectroscopy of Hydrous Magnesium Silicates: Evidence for Proton Dynamics. Journal of Physical Chemistry C, 2009, 113, 465-471.	1.5	61
132	Multinuclear Magnetic Resonance and DFT Studies of the Poly(chlorotrifluoroethylene- <i>alt</i> -ethyl vinyl ether) Copolymers. Macromolecules, 2009, 42, 5652-5659.	2.2	42
133	Spin-locking of half-integer quadrupolar nuclei in nuclear magnetic resonance of solids: Second-order quadrupolar and resonance offset effects. Journal of Chemical Physics, 2009, 131, 194509.	1.2	48
134	Transformation of AlPO-53 to JDF-2: Reversible Dehydration of a Templated Aluminophosphate Studied by MAS NMR and Diffraction. Journal of Physical Chemistry C, 2009, 113, 10780-10789.	1.5	40
135	Early Stage Reversed Crystal Growth of Zeolite A and Its Phase Transformation to Sodalite. Journal of the American Chemical Society, 2009, 131, 17986-17992.	6.6	129
136	Recent advances in solid-state NMR spectroscopy of quadrupolar nuclei. Physical Chemistry Chemical Physics, 2009, 11, 6892.	1.3	114
137	Cation Disorder in Pyrochlore Ceramics: ⁸⁹ Y MAS NMR and First-Principles Calculations. Journal of Physical Chemistry C, 2009, 113, 18874-18883.	1.5	62
138	Control of polymorphism in NaNbO3by hydrothermal synthesis. Chemical Communications, 2009, , 68-70.	2.2	65
139	DFT calculations of quadrupolar solidâ€state NMR properties: Some examples in solidâ€state inorganic chemistry. Journal of Computational Chemistry, 2008, 29, 2279-2287.	1.5	52
140	Structure and NMR assignment in calcined and as-synthesized forms of AlPO-14: a combined study by first-principles calculations and high-resolution 27Al–31P MAS NMR correlation. Physical Chemistry Chemical Physics, 2008, 10, 5754.	1.3	95
141	First-principles calculations of solid-state17O and29Si NMR spectra of Mg2SiO4polymorphs. Physical Chemistry Chemical Physics, 2007, 9, 1587-1598.	1.3	65
142	17O and29Si NMR Parameters of MgSiO3Phases from High-Resolution Solid-State NMR Spectroscopy and First-Principles Calculations. Journal of the American Chemical Society, 2007, 129, 13213-13224.	6.6	104
143	89Y Magic-Angle Spinning NMR of Y2Ti2-xSnxO7Pyrochlores. Journal of Physical Chemistry B, 2006, 110, 10358-10364.	1.2	47
144	Solid state170 NMR—an introduction to the background principles and applications to inorganic materials. Chemical Society Reviews, 2006, 35, 718-735.	18.7	203

#	Article	IF	CITATIONS
145	Nuclear Overhauser Effect (NOE) Enhancement of 11B NMR Spectra of Borane Adducts in the Solid State. Journal of the American Chemical Society, 2006, 128, 6782-6783.	6.6	17
146	Characterisation of the (Y1â^'xLax)2Ti2O7system by powder diffraction and nuclear magnetic resonance methods. Journal of Materials Chemistry, 2006, 16, 4665-4674.	6.7	26
147	Dynamics on the Microsecond Timescale in Microporous Aluminophosphate AlPO-14 as Evidenced by27Al MQMAS and STMAS NMR Spectroscopy. Journal of the American Chemical Society, 2006, 128, 8054-8062.	6.6	72
148	2H double-quantum MAS NMR spectroscopy as a probe of dynamics on the microsecond timescale in solids. Chemical Physics Letters, 2006, 423, 276-281.	1.2	58
149	STARTMAS: A MAS-based method for acquiring isotropic NMR spectra of spin I=3/2 nuclei in real time. Chemical Physics Letters, 2006, 431, 390-396.	1.2	13
150	23Na multiple-quantum MAS NMR of the perovskites NaNbO3and NaTaO3. Physical Chemistry Chemical Physics, 2006, 8, 3423-3431.	1.3	86
151	Structural information from quadrupolar nuclei in solid state NMR. Concepts in Magnetic Resonance Part A: Bridging Education and Research, 2006, 28A, 183-248.	0.2	136
152	Correlating fast and slow chemical shift spinning sideband patterns in solid-state NMR. Journal of Magnetic Resonance, 2005, 174, 301-309.	1.2	32
153	Rotor-synchronized acquisition of quadrupolar satellite-transition NMR spectra: practical aspects and double-quantum filtration. Journal of Magnetic Resonance, 2005, 177, 44-55.	1.2	26
154	High-resolution 170 MAS NMR spectroscopy of forsterite (Â-Mg2SiO4), wadsleyite (Â-Mg2SiO4), and ringwoodite (Â-Mg2SiO4). American Mineralogist, 2005, 90, 1861-1870.	0.9	24
155	Solid-state 17O nuclear magnetic resonance spectroscopy without isotopic enrichment: direct detection of bridging oxygen in radiation damaged zircon. Solid State Nuclear Magnetic Resonance, 2004, 26, 105-112.	1.5	29
156	High-Resolution NMR of Quadrupolar Nuclei in Solids: The Satellite-Transition Magic Angle Spinning (STMAS) Experiment. ChemInform, 2004, 35, no.	0.1	0
157	High-resolution NMR of quadrupolar nuclei in solids: the satellite-transition magic angle spinning (STMAS) experiment. Progress in Nuclear Magnetic Resonance Spectroscopy, 2004, 45, 53-108.	3.9	133
158	Spin-locking of half-integer quadrupolar nuclei in nuclear magnetic resonance of solids: Creation and evolution of coherences. Journal of Chemical Physics, 2004, 120, 2719-2731.	1.2	31
159	Satellite-Transition MAS NMR of Low-Î ³ Nuclei at Natural Abundance:Â Sensitivity, Practical Implementation, and Application to39K (I= 3/2) and25Mg (I= 5/2). Journal of Physical Chemistry B, 2004, 108, 13292-13299.	1.2	29
160	SCAM-STMAS: satellite-transition MAS NMR of quadrupolar nuclei with self-compensation for magic-angle misset. Journal of Magnetic Resonance, 2003, 162, 402-416.	1.2	16
161	High-Resolution 170 NMR Spectroscopy of Wadsleyite (β-Mg2SiO4). Journal of the American Chemical Society, 2003, 125, 11824-11825.	6.6	34
162	Relative Orientation of Quadrupole Tensors from High-Resolution NMR of Powdered Solids. Journal of Physical Chemistry A, 2002, 106, 9470-9478.	1.1	32

#	Article	IF	CITATIONS
163	170 Multiple-Quantum MAS NMR Study of Pyroxenes. Journal of Physical Chemistry B, 2002, 106, 773-778.	1.2	37
164	High-Resolution NMR Spectroscopy of Quadrupolar Nuclei in Solids:  Satellite-Transition MAS with Self-Compensation for Magic-Angle Misset. Journal of the American Chemical Society, 2002, 124, 11602-11603.	6.6	24
165	A multiple-quantum 23Na MAS NMR study of amorphous sodium gallium silicate zeolite precursors. Journal of Materials Chemistry, 2002, 12, 1469-1474.	6.7	21
166	Satellite-Transition MAS NMR of Spin I=3/2, 5/2, 7/2, and 9/2 Nuclei: Sensitivity, Resolution, and Practical Implementation. Journal of Magnetic Resonance, 2002, 156, 269-281.	1.2	71
167	Motional broadening: an important distinction between multiple-quantum and satellite-transition MAS NMR of quadrupolar nuclei. Chemical Physics Letters, 2002, 364, 634-642.	1.2	67
168	170 Multiple-Quantum MAS NMR Study of High-Pressure Hydrous Magnesium Silicates. Journal of the American Chemical Society, 2001, 123, 6360-6366.	6.6	39
169	Relative Orientation of Quadrupole Tensors from Two-Dimensional Multiple-Quantum MAS NMR. Journal of the American Chemical Society, 2001, 123, 8135-8136.	6.6	35
170	Novel two-dimensional NMR methods that combine single-quantum cross-polarization and multiple-quantum MAS of quadrupolar nuclei. Chemical Physics Letters, 2001, 340, 500-508.	1.2	20
171	Two-dimensional satellite-transition MAS NMR of quadrupolar nuclei: shifted echoes, high-spin nuclei and resolution. Chemical Physics Letters, 2001, 345, 400-408.	1.2	31
172	Multiple-Quantum Cross-Polarization and Two-Dimensional MQMAS NMR of Quadrupolar Nuclei. Journal of Magnetic Resonance, 2000, 147, 238-249.	1.2	52
173	Multiple-quantum MAS NMR of quadrupolar nuclei. Do five-, seven- and nine-quantum experiments yield higher resolution than the three-quantum experiment?. Solid State Nuclear Magnetic Resonance, 2000, 16, 203-215.	1.5	100
174	Single- and multiple-quantum cross-polarization in NMR of quadrupolar nuclei in static samples. Molecular Physics, 2000, 98, 1-26.	0.8	42
175	Reply to Comment on "27Al Multiple-Quantum Magic Angle Spinning NMR Study of the Thermal Transformation between the Microporous Aluminum Methylphosphonates AlMePO-β and AlMePO-α― Journal of Physical Chemistry B, 2000, 104, 9767-9767.	1.2	0
176	27Al Multiple-Quantum Magic Angle Spinning NMR Study of the Thermal Transformation between the Microporous Aluminum Methylphosphonates AlMePO-β and AlMePO-α. Journal of Physical Chemistry B, 1999, 103, 812-817.	1.2	30
177	Three- and five-quantum ¹⁷ O MAS NMR of forsterite Mg ₂ SiO ₄ . American Mineralogist, 1999, 84, 1191-1194.	0.9	37
178	Multiple-quantum cross-polarization in MAS NMR of quadrupolar nuclei. Chemical Physics Letters, 1998, 288, 509-517.	1.2	52